A family of models of hard and soft interfaces with damage

Frédéric Lebon, Maria Letizia Raffa, Raffaella Rizzoni

▶ **To cite this version:**

Frédéric Lebon, Maria Letizia Raffa, Raffaella Rizzoni. A family of models of hard and soft interfaces with damage. Theoretical and Applied Fracture Mechanics, 2023, 127, pp.104008. 10.1016/j.tafmec.2023.104008 . hal-04385255

HAL Id: hal-04385255
https://hal.science/hal-04385255v1

Submitted on 29 Dec 2024

HAL is a multi-disciplinary open access archive for the deposit and dissemination of scientific research documents, whether they are published or not. The documents may come from teaching and research institutions in France or abroad, or from public or private research centers.

L'archive ouverte pluridisciplinaire **HAL**, est destinée au dépôt et à la diffusion de documents scientifiques de niveau recherche, publiés ou non, émanant des établissements d'enseignement et de recherche français ou étrangers, des laboratoires publics ou privés.

Distributed under a Creative Commons Attribution - NonCommercial 4.0 International License

Accepted Manuscript

A Family of Models of Hard and Soft Interfaces with Damage

Frédéric Lebon[a,*], Maria Letizia Raffa[b] and Raffaella Rizzoni[c]

[a]Aix-Marseille Univ., CNRS, Centrale Marseille, LMA, 4 Impasse Nikola Tesla, CS40006, Marseille, 13453 Cedex 13, France [b]Laboratoire QUARTZ EA 7393, ISAE-Supméca, 3 Rue Fernand Hainaut, Saint-Ouen-sur-Seine, 93400 Cedex, France
[c]Department of Engineering, University of Ferrara, Via Saragat 1, Ferrara, 44122, Italy

ARTICLE INFO

Keywords:
Adhesive bonding
Imperfect interface
Cracks density
Damage
Damage velocity

ABSTRACT

In many industrial applications in aeronautical, civil, energetic, automotive and biomedical engineering, adhesion techniques have recently emerged as assembly procedures alternative to conventional joining. Adhesive bonding is advantageous for many aspects, such as mitigation of stress concentration, better resistance to corrosion and water sealing, and the possibility of assembly dissimilar materials. In the literature, interface models are a classical modeling approach to the description of the mechanical behavior of adhesive joints. In this paper, an original generalized interface model is presented for both soft and hard adhesives, characterized by lower and higher stiffness than the adherents, respectively. The proposed model is able to capture a damaging behavior of the adhesive material, the elastic properties of which are obtained by homogenizing a microcracked media. The cracks density in the adhesive is the damage parameter, and a kinetic law based on the generalized standard material model describes its evolution. The role and relevance of damage velocity is illustrated through some simple examples and with a comparison with experimental data taken from literature. The numerical results show how the mechanical properties of the adhesive and the joint degrade as damage evolves, indicating a transition from quasi-brittle to brittle behavior as the damage velocity decreases.

1. Introduction

In recent decades, increasingly industrial applications employ bonding as a common joining technique. Some examples are GFRP pultruded beams in civil engineering Ascione, Mancusi, Spadea, Lamberti, Lebon and Maurel-Pantel (2015); Lamberti, Maurel-Pantel, Ascione and Lebon (2016); Orefice, Mancusi, Dumont and Lebon (2016), composites Budhe, Banea and de Barros (2018); Kupski and de Freitas (2021) or direct bonding in aerospace engineering, ship hulls in marine engineering Delzendehrooy, Akhavan-Safar, Barbosa, Beygi, Cardoso, Carbas, Marques and da Silva (2022); Amaechi, Chesterton, Butler, Wang and Ye (2021), orthopedic Weber and Chapman (1984); Farrar (2012) or dental implants Maurer, Bekes, Gernhardt, Schaller and Schubert (2004); Meerbeek, Peumans, Poitevin, Mine, Ende, Neves and Munck (2010) in biomedical engineering.

Bonding has emerged as an alternative to traditional joining techniques, such as welding and riveting, due to several favourable features, e.g. mitigation of stress concentration, better resistance to corrosion and water sealing, and the possibility of joining dissimilar materials.

*Corresponding author
lebon@lma.cnrs-mrs.fr (F. Lebon); maria-letizia.raffa@isae-supmeca.fr (M.L. Raffa); raffaella.rizzoni@unife.it (R. Rizzoni)
http://www.lma.cnrs-mrs.fr/spip.php?auteur83&lang=fr (F. Lebon); https://www.quartz-lab.fr/raffa-maria-letizia (M.L. Raffa); https://docente.unife.it/raffaella.rizzoni (R. Rizzoni)
ORCID(s): 0000-0001-8271-5314 (F. Lebon); 0000-0002-4062-7153 (M.L. Raffa); 0000-0003-4962-7878 (R. Rizzoni)

In addition, bonding is increasingly used in the transportation industry because it allows the production of lightweight structures, leading to reduced CO_2 emissions. Despite this, there are disadvantages.

Under service conditions, durability is a major concern limiting the use of adhesives in structural applications. Indeed, corrosion and aging can cause microcracking phenomena that can be measured by non-destructive techniques. An additional disadvantage is the multifactorial and multiscale nature of the damage phenomenon in adhesive joints, which complicates validation and implementation of reliable prognostic approaches.

In adhesives, the stress-strain diagram in tension or shear typically exhibits an initially linear elastic phase followed by collapse (brittle fracture) or softening and collapse (ductile fracture), see Chaves, da Silva, de Moura, Dillard and Esteves (2014); Budzik, Wolfahrt, Reis, Kozlowski, Sena-Cruz, Papadakis, Saleh, Machalicka, de Freitas and Vassilopoulos (2021). The cyclic behavior often exhibits hysteresis loops (Orefice et al. (2016); Lamberti, Maurel-Pantel, Lebon and Ascione (2022)).

Non-linearity of mechanical response indicates the presence of a microcracking process, especially in the brittle case: pre-existing microcracks introduced during adhesive preparation (manufacturing, heat treatment, etc.) are initially present in the linear elastic phase and propagate during softening, leading to debonding and cracking.

An additional difficulty is related to the stiffness of the adhesive, varying from MPa to GPa depending on the industrial manufacturing process. In this paper, we propose a model for the mechanical behavior of adhesive joints able to account for these different aspects of complexity.

Computationally, the mechanical modeling of adhesives is complicated by the smallness of their thickness, leading

Accepted Manuscript

to a very fine mesh, increased degrees of freedom and ill-conditioning.

One possible simplifying approach is to use surface models. The most popular strategy for modeling damage in adhesives is based on cohesive zone models (CZMs) Ramalho, Campilho, Belinha and Silva (2020), typically described by a traction-separation law prescribed across the cohesive surface.

Deductive interface models based on asymptotic theory are a viable alternative to cohesive phenomenological models. Deductive models are obtained by introducing asymptotic expansions of the relevant fields dependent on a small parameter (the thickness of the adhesive) into the equations of the equilibrium problem and by studying the limit problem when the parameter tends to zero Benveniste and Miloh (2001); Dumont, Lebon, Raffa and Rizzoni (2017); Furtsev and Rudoy (2020); Rizzoni, Dumont, Lebon and Sacco (2014); Licht, Orankitjaroen and Weller (2022); Geymonat, Krasucki and Lenci (1999); Serpilli and Lenci (2012a,b). In the limit configuration, the adhesive is replaced by a surface whose properties are characterized by those of the original adhesive material (stiffness, kinematics, viscosity, inertia, damage properties, etc.). Larger complexity of the material model yields higher accuracy of the deductive surface model. Deductive interface models can be successfully applied in continuum numerical methods using joint-element techniques, and they can be very useful for the stress analysis of complicated structural components, see for example Ascione et al. (2015); Lamberti et al. (2016); Orefice et al. (2016); Lamberti et al. (2022).

In structural bonding, damage with microfracture evolution is generally observed Lamberti et al. (2022). As already proposed in previous works, the density of microcracks can be considered as the damage variable Maurel-Pantel, Lamberti, Raffa, Suarez, Ascione and Lebon (2019); Bonetti, Bonfanti, Lebon and Rizzoni (2017). The purpose of the present work is to propose an interface model with damage evolution able to account for non-local effects as described in the literature Hochard, Payan and Bordreuil (2006); Hochard, Lahellec and Bordreuil (2007).

With respect to previous work of the authors Raffa, Rizzoni and Lebon (2021); Raffa, Lebon and Rizzoni (2022), in this paper we introduce a damage velocity parameter as an element of novelty. This parameter is related to the exponent of the dissipation potential, which is usually assumed to be quadratic. We show that more general potentials induce joint stress-strain responses characterized by different types of damage. In particular, as the damage rate (the exponent) decreases, a transition from quasi-fragile to brittle behavior emerges.

The structure of the paper is the following. In Section 2, we introduce a general analytical model of damaging material. The model accounts for damage evolution and non-local effects. Section 3 is dedicated to the derivation of the interface model and two different cases are considered: the case of soft adhesive material and the case of hard adhesive material. In Section 4, we present a parametric analysis whose results show the influence of the damage parameters on the stress-strain response of the adhesive and of the joint. A comparison with some experimental data taken from the literature indicates that introducing the damage velocity allows an improved description of the experimental findings. Finally, in Section 5, conclusions and some insight for further study are provided.

2. A general model of damaging material

In the following, a thermodynamically-consistent formulation for an elastic adhesive with damage is derived. It is well-known that the choice of state variables is subjective, depending on the studied phenomenon. In the proposed model, the following variables have been chosen:

- The elastic strain tensor $e(u)$, where u is the displacement field (under the small perturbations hypothesis).
- A variable denoted R, which is a cracks density and represents here an internal state variable of damage.

Hereafter, the process will be considered as isothermal. The thermodynamic state of the material will then be represented locally by a potential depending on these state variables. A "specific free energy" potential $\psi(e(u), R)$ is chosen as:

$$\psi\left(e\left(u\right), R\right) = \frac{1}{2}\,\mathbb{K}(R)\,e(u) : e(u) + \omega(R) + \frac{\alpha}{p}|\nabla R|^p + I_{[0,1]}(R) \tag{1}$$

where $\mathbb{K}(R)$ is the stiffness tensor of the material (with usual symmetry and positivity properties), $|.|$ is the Euclidean norm, α and p are material parameters, and I_A is the indicator function of the set A defined as follows:

$$\begin{aligned} &I_A(x) = 0 \quad \text{if } x \in A, \\ &I_A(x) = +\infty \quad \text{if } x \notin A. \end{aligned} \tag{2}$$

The indicator function is used to force the damage variable to remain in the range $[0, 1]$. The function $\omega(R) > 0$ can be seen as an activation energy of the damage, cf. Raffa et al. (2022). The dependence of $\mathbb{K}(R)$ and $\omega(R)$ on the damage variable R will be specified in the following. The term $|\nabla R|^p$ models a non-local character of the damage.

Classically, the stress field σ and the thermodynamic force χ associated with the damage variable are derived as

$$\begin{aligned} &\sigma = \psi_{,e(u)} = \mathbb{K}(R)\,e(u) \\ &\chi \in \partial_R \psi \end{aligned} \tag{3}$$

where $(.)_{,e(u)}$ denotes the partial derivation with respect to $e(u)$ and ∂_R denotes the subdifferential of ψ with respect to the damage variable R.

As is well known, the thermodynamic potential $\psi(e(u), R)$ links the state variables $(e(u), R)$ and their associated variables (σ, χ), at a given time. On the other hand, this datum

Table 1
List of parameters and functions defining the damage evolution.

Parameters	Unity	Interpretation
β	no unit	damage velocity
p	no unit	non-local parameter
α	Pa·m^p	non-local effect parameter
ω	Pa	activation energy
η	Pa·s	viscosity
$\mathbb{K}$	Pa	stiffness tensor

does not allow to write the evolution of these variables during a transformation. This evolution will be given by a complementary law: the additional constitutive equation of the material. To describe the evolution of the state variables during the transformation, while respecting the second principle of thermodynamics, we postulate the existence of a dissipation potential ϕ, expressed as a continuous scalar function of the "flux" variables, i.e. $\phi(\dot{R})$. This potential must be positive and zero at the origin. It is often chosen convex even though this is not essential. In this study, the potential is chosen as

$$\phi(\dot{R}) = \frac{1}{\beta+1}\eta(R)\dot{R}^{\beta+1} + I_{[0,+\infty[}(\dot{R}), \tag{4}$$

where β and $\eta > 0$ are two material parameters. The first one allows to control damage velocity. The second one, which depends *a priori* on the damage variable, can be see as a viscosity parameter. The indicator function is used to force the damage to be irreversible. The "dual" variable will then be obtained from the following complementary law

$$\chi \in -\partial_{\dot{R}}\phi. \tag{5}$$

Combining the previous equations, the following damage evolution equation is obtained:

$$\begin{aligned} 0 \in & \eta(R)R^{\beta} + \frac{1}{2}\mathbb{K}_{,R}e(u)e(u) + \omega_{,R}(R) \\ & + \alpha\Delta_p R + \partial_R I_{[0,1]}(R) + \partial_{\dot{R}} I_{[0,+\infty[}(\dot{R}), \end{aligned} \tag{6}$$

where Δ_p denotes the p-Laplacian operator

$$\Delta_p R = \nabla.(|\nabla R|^{p-2}\nabla R). \tag{7}$$

Introducing an initial condition, this evolution law can be expressed as

$$\begin{aligned} \eta(R)\dot{R}^{\beta} = & -\left\{\omega_{,R}(R) + \frac{1}{2}\mathbb{K}_{,R}(R)e(u)e(u) + \alpha\Delta_p R\right\}_-, \\ & R(0) = R_0, \end{aligned} \tag{8}$$

where $()_-$ denotes the negative part of a function.

In conclusion, the model depends on the material parameters listed in Table 1. Note that these parameters can depend or not on the cracks density R.

3. Derivation of the interface model

In this Section, we obtain the interface model by applying the method of asymptotic expansions. In Subsection 3.1, we introduce the main notation and the equilibrium problem of the joint configuration. Subsection 3.2 is devoted to the asymptotic analysis, based on power asymptotic expansions of the stresses and the displacements fields in the adherents and in the adhesive. Two cases are then considered: the case of hard adhesive material, with fixed elasticity constants, is treated in Subsection 3.2.1; the case of soft adhesive material, with elasticity constants rescaling like the small parameter, is addressed in Section 3.2.2.

3.1. Notation and problem statement

An adhesive joint is geometrically described as two solids (the adherents) in perfect contact with a thin layer (the adhesive) of constant thickness t_h, as shown in Fig. 1. The adhesive occupies a domain B_ε in $\mathbb{R}^3$ with cross-section S, being S an open bounded set in $\mathbb{R}^2$ with a smooth boundary. A Cartesian coordinate system is introduced, with origin O on S, (x_1, x_2, x_3) the three coordinates of a particle, and $(\mathbf{e}_1, \mathbf{e}_2, \mathbf{e}_3)$ an orthonormal base vectors. The domain S is a planar surface belonging to the plane $(O, \mathbf{e}_1, \mathbf{e}_2)$.

We define the non-negative thickness ratio $\varepsilon = t_h/L \ll 1$, with L a representative length scale of the adherents. In the following formulation, the ratio ε will denote the small parameter of the asymptotic analysis. The adherents are assumed to occupy the reference configurations $\Omega_\varepsilon^{\pm} \subset \mathbb{R}^3$. $S_\varepsilon^{\pm}$ in $\mathbb{R}^2$ denote the planar interfaces between the adhesive and the adherents, and $\Omega = \Omega_\varepsilon^{\pm} \cup S_\varepsilon^{\pm} \cup B_\varepsilon$ is the whole joint configuration. The stresses and the displacements fields are taken to be continuous across $S_\varepsilon^{\pm}$.

In the limit of a vanishing ε, the adhesive is geometrically replaced by a surface across which certain conditions on the displacements and the tractions prevail, cf. Dumont et al. (2017). The technique based on matched asymptotic expansions is a traditional method to obtain such transmission conditions, representing, in the form of imperfect contact laws, the limiting behavior of a very thin adhesive, see for example Geymonat et al. (1999); Serpilli and Lenci (2012b); Dumont et al. (2017).

The materials composing the various parts of the joint are taken to be homogeneous and linearly elastic, with $\mathbb{A}^{\pm}$ be the fourth-rank elasticity tensors of the adherents, and $\mathbb{K}$ the elasticity tensor of the adhesive. The damaging constitutive behavior of the adhesive has already been introduced in Section 2. Note that, the material parameters of the adhesive, summarized in Table 1, are assumed to depend on ε, as in Bonetti et al. (2017); Maitlo, Lebon and Bauzet (2019). The elasticity tensors $\mathbb{A}^{\pm}$ have the usual symmetry properties, with the minor and major symmetries, and are positive definite, but otherwise can have arbitrary material symmetries (anisotropy). A body force density $\mathbf{f}^{\pm}$ is applied in $\Omega^{\pm}$, and a surface force density $\mathbf{g}^{\pm}$ on a part Γ_g of the boundary of the two adherents. In the adhesive, external forces are neglected. On a part Γ_u of the boundary, homogeneous boundary conditions can be assigned.

Accepted Manuscript

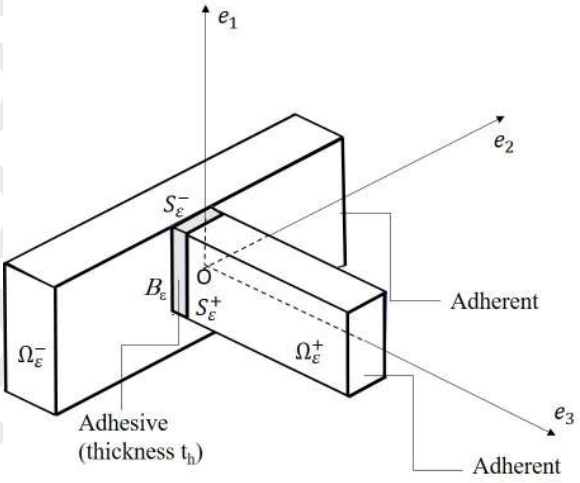

Figure 1: Initial problem of bonding (adhesive in grey, adherents in white).

3.2. Asymptotic analysis

In the following, these assumptions are made:

- Without loss of generality, the model parameters (see Table 1) are assumed to be independent of the direction perpendicular to the adhesive plane. More complex scenarios have been considered in Maitlo et al. (2019).
- Parameters β and p are independent of the relative thickness ε.
- Parameters η, ω and α depend now on the relative thickness ε as : $\eta(\varepsilon) = \tilde{\eta}\,\varepsilon^{-1}$, $\omega(\varepsilon) = \tilde{\omega}\,\varepsilon^{-1}$ and $\alpha(\varepsilon) = \tilde{\alpha}\,\varepsilon^{-1}$. The dependency of $\mathbb{K}$ on ε will be investigated in what follows.

The method of matched asymptotic expansions can be briefly schematized as follows.

- The displacements and the stresses fields are expanded with respect to the thickness ratio ε:

$$\sigma^\varepsilon = \sigma^0 + \varepsilon\sigma^1 + o(\varepsilon), \tag{9}$$
$$u^\varepsilon = u^0 + \varepsilon u^1 + o(\varepsilon). \tag{10}$$

- A change of variables is introduced: the adhesive is rescaled along $\mathbf{e}_3$ becoming of unit length, cf. Fig.2. Correspondingly, the adherents are translated relatively along $\mathbf{e}_3$. The final domain is now independent of ε, and the thickness parameter ε is transferred to the operators.
- The rescaled fields are transferred to the equilibrium and constitutive equations, and the terms at the various orders are identified. In the present paper, only the first and the second terms of the expansions are identified (higher orders are neglected).
- A matching condition is introduced to relate the interface law to the boundary configuration obtained for a vanishing adhesive thickness (cf. Fig. 3).

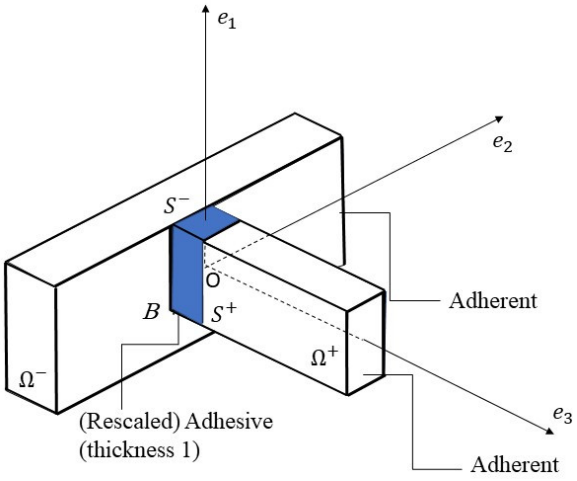

Figure 2: Sketch of the asymptotic study (rescaled adhesive in blue).

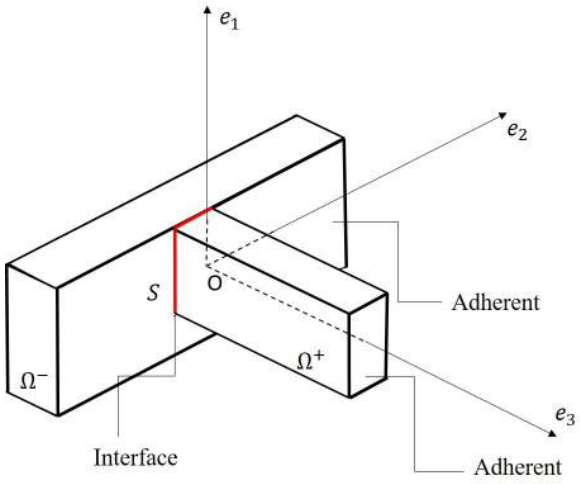

Figure 3: Final configuration.

We introduce the following notation:

- $[[f]] := f(\mathbf{x}_\gamma, 0^+) - f(\mathbf{x}_\gamma, 0^-)$: jump in the limit configuration (see Fig. 3);
- $\langle\langle f \rangle\rangle := \frac{1}{2}\{f(\mathbf{x}_\gamma, 0^+) + f(\mathbf{x}_\gamma, 0^-)\}$: average in the limit configuration (see Fig. 3);

where f is a generic function, $\mathbf{x}_\gamma = (x_1, x_2)$, and Greek indexes ($\gamma, \delta = 1, 2$) are related to the in-plane (x_1, x_2) coordinates.

Accepted Manuscript

Accepted Manuscript

3.2.1. The case of similar stiffness: hard interface

We now consider an adhesive material whose stiffness is comparable to that of the adherents. An adhesive with this characteristic gives rise to a *hard* interface. Mathematically, this is equivalent to assuming that the elastic tensor of the adhesive material is independent of ε

$$\mathbb{K}^\varepsilon = \mathbb{K}. \tag{11}$$

In the following, the matrices K^{jl}, for $j,l = 1,2,3$, are defined such that $K^{jl}_{ki} := \mathbb{K}_{ijkl}$, with $i,k = 1,2,3$. In this case, the following first- and second-order transmission conditions are obtained.

- Zero-order interface law:

$$[[\mathbf{u}^0]] = \mathbf{0}, \tag{12}$$
$$[[\sigma^0\,\mathbf{i}_3]] = \mathbf{0}. \tag{13}$$

- First-order interface law:

$$[[\mathbf{u}^1]] = (K^{33})^{-1}\left(\sigma^0\mathbf{i}_3 - K^{\gamma 3}\mathbf{u}^0_{,\gamma}\right) - \langle\langle \mathbf{u}^0_{,3}\rangle\rangle. \tag{14}$$

$$[[\sigma^1\,\mathbf{i}_3]] = -\left(K^{3\gamma}(K^{33})^{-1}\left(\sigma^0\mathbf{i}_3 - K^{\delta 3}\mathbf{u}^0_{,\delta}\right)\right)_{,\gamma} - \left(K^{\delta\gamma}\mathbf{u}^0_{,\delta}\right)_{,\gamma} - \langle\langle \sigma^0_{,3}\mathbf{i}_3\rangle\rangle. \tag{15}$$

Introducing the approximation

$$\mathbf{u}^\varepsilon \approx \mathbf{u}^0 + \varepsilon\mathbf{u}^1, \tag{16}$$
$$\sigma^\varepsilon \approx \sigma^0 + \varepsilon\sigma^1, \tag{17}$$

and using the parameter rescaling as proposed in Maitlo et al. (2019); Raffa et al. (2022), the following damage evolution equation can be obtained

$$\tilde{\eta}(R)\dot{R}^\beta = -\left\{\tilde{\omega}_{,R}(R) + \frac{1}{2}\,\mathbf{K}^\varepsilon_{,R}(R)\begin{pmatrix}\langle\langle \mathbf{u}^\varepsilon_{,1}\rangle\rangle\\ \langle\langle \mathbf{u}^\varepsilon_{,2}\rangle\rangle\\ [[\mathbf{u}^\varepsilon]] + \varepsilon\langle\langle \mathbf{u}^\varepsilon_{,3}\rangle\rangle\end{pmatrix}\cdot\begin{pmatrix}\langle\langle \mathbf{u}^\varepsilon_{,1}\rangle\rangle\\ \langle\langle \mathbf{u}^\varepsilon_{,2}\rangle\rangle\\ [[\mathbf{u}^\varepsilon]] + \varepsilon\langle\langle \mathbf{u}^\varepsilon_{,3}\rangle\rangle\end{pmatrix} + \tilde{\alpha}\Delta_p^2\,R\right\}_- \tag{18}$$

where the matrix $\mathbf{K}^\varepsilon$ takes the form

$$\mathbf{K}^\varepsilon = \begin{pmatrix}\varepsilon K^{11} & \varepsilon K^{12} & K^{13}\\ \varepsilon K^{12} & \varepsilon K^{22} & K^{23}\\ K^{13} & K^{23} & \frac{1}{\varepsilon}K^{33}\end{pmatrix}, \tag{19}$$

and Δ_p^2 denotes the p-Laplacian on the surface S.

3.2.2. The case of non similar stiffness: soft interface

The second case studied is for a *soft* adhesive, composed of a material with lower stiffness than that of adherents. To simulate such characteristic, the elasticity tensor of the adhesive is assumed to rescale with ε, as follows:

$$\mathbb{K}^\varepsilon = \varepsilon\mathbb{K}. \tag{20}$$

For the sake of simplicity, only the results at the lower order are presented. The interface law is thus of spring-type, characterized by the continuity of the traction vector and by a jump discontinuity of the displacement vector:

$$\sigma^0\,\mathbf{i}_3 = \mathbb{K}[[\mathbf{u}^0]], \tag{21}$$
$$[[\sigma^0\,\mathbf{i}_3]] = \mathbf{0}. \tag{22}$$

Introducing the zero-order approximation

$$\mathbf{u}^\varepsilon \approx \mathbf{u}^0, \tag{23}$$
$$\sigma^\varepsilon \approx \sigma^0, \tag{24}$$

the damage evolution equation now takes the form

$$\tilde{\eta}(R)\dot{R}^\beta = -\left\{\tilde{\omega}_{,R}(R) + \frac{1}{2}\,\mathbf{K}^{33}_{,R}(R)[[u^\varepsilon]][[u^\varepsilon]] + \tilde{\alpha}\Delta_p^2 R\right\}_-. \tag{25}$$

Equations (18) and (25) are integrated with the initial condition $R(0) = R_0$, being R_0 the initial value of the cracks density.

4. A parametric analysis

In this section, a parametric study on damage model parameters is proposed. To this aim, two simple 1D formulations are considered in both bulk and joint configuration for the damaged adhesive material. In the 1D configuration, the damage evolution law becomes soft and the p-Laplacian vanishes. Experimental data from Murakami, Sekiguchi, Sato, Yokoi and Furusawa (2016) on a quasi-brittle epoxy adhesive (Denatite 2204, Nagase ChemteX Co., Ltd., Osaka, Japan) have been used for comparison.

4.1. Bulk adhesive configuration

By specializing Eq. (8) to the 1D case, the damage evolution law reads as:

$$\eta(R)\dot{R}^\beta = -\left\{\omega_{,R}(R) + \frac{1}{2}\,E_{,R}(R)\,\epsilon^2\right\}_- \tag{26}$$

where ϵ is the uniaxial strain and $E_{,R}(R)$ represents the derivative with respect to R of the Young's modulus of the damaged adhesive. Under the assumption of a damaged material as defined in Welemane and Goidescu (2010), by a particular homogenization process, it is obtained:

$$E(R) = E_0\,(1 - 2\pi\,R), \quad E_{,R}(R) = -2\pi\;E_0 \tag{27}$$

where E_0 represents the Young's modulus of the undamaged material. For the numerical simulation, a linear strain ramp

is imposed, $\epsilon(t) = \dot{\epsilon} t$, with $\dot{\epsilon}$ the strain rate. Accordingly, the damage evolution equation can be rewritten in the form

$$\dot{R} = -\frac{1}{\eta(R)} \left\{ \omega_{,R}(R) - \pi E_0 \dot{\epsilon}^2 t^2 \right\}_-^{\frac{1}{\beta}} \quad \text{for } \beta \neq 0 \quad (28)$$

In what follows, it is assumed that $\omega_{,R}(R)$ and $\eta(R)$ are constant parameters, equal to $\omega_{,R}(R) = \bar{\omega} = 0.06$ Pa, $\eta(R) = \bar{\eta} = 3.6 \cdot 10^2$ Pa·s and $R_0 = 0$. A parametric study is carried out here on the damage velocity β. For a complete study on the influence of parameters $\bar{\omega}$ (activation energy threshold) and $\bar{\eta}$ (damage viscosity) one could refer to Raffa et al. (2022). Damage initiates when:

$$t = \frac{1}{\dot{\epsilon}} \left(\frac{\bar{\omega}}{\pi E_0} \right)^{\frac{1}{2}} = 2.7, \quad (29)$$

where t represents a normalized time. Figure 4 shows the evolution of the cracks density R as a function of the normalized time. The various curves are obtained by integrating Eq. (28) for different values of the damage velocity β. Figure

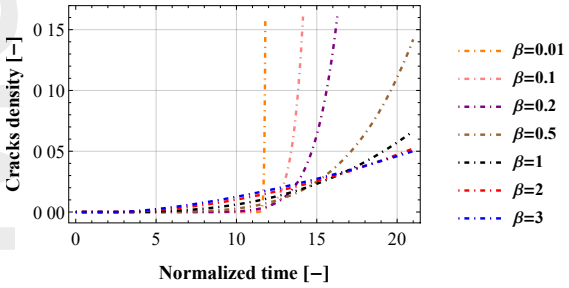

Figure 4: Influence of the damage velocity β: Evolution of the cracks density R as a function of the normalized time.

4 highlights that the parameter β governs the rate dependency of the damage phenomenon. In detail, all curves have the same activation energy threshold $\bar{\omega}$, which means that damage begins at the same time, thus one can conclude that the smaller the parameter β, the faster the damage evolves. This aspect is also supported by the behaviour of the Young's modulus of the damaged material, shown in Fig. 5.

The evolution of the Young's modulus of an adhesive (bulk) during a tensile test was extrapolated from experimental data by Murakami et al. (2016), normalized with respect to the modulus of the undamaged material and compared with the proposed numerical results. It is found that the damage velocity β is suitable to reproduce the degradation of mechanical properties due to damage in quasi-brittle adhesive, as Denatite 2204. In particular, for $\beta = 3$ a very good agreement between experimental and numerical curves is found. In fact, in the case of $\beta = 1$ (black curve in Fig. 5), which corresponds to the damage evolution law proposed by Raffa et al. (2022), this phenomenon is not well described. Figure 6 shows the global response (tensile stress-strain) during the same tensile test by Murakami et al.

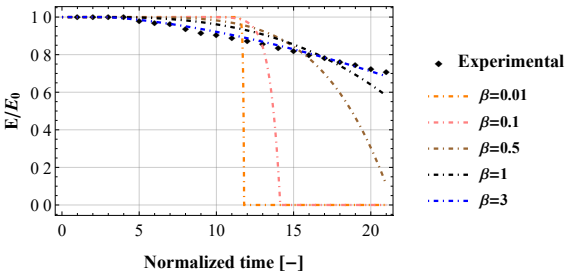

Figure 5: Influence of the damage velocity β: Evolution of the dimensionless Young's modulus of the damaged adhesive as a function of the normalized time. A comparison with the experimental data from Murakami et al. (2016) is presented.

(2016) on the bulk specimen of Denatite 2204. Also in this case, experimental data are compared with the numerical results for a varying damage velocity, and for $\beta = 3$ a good agreement is confirmed.

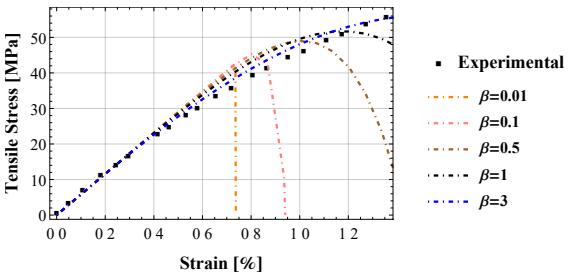

Figure 6: Influence of the damage velocity β: Tensile test behavior of the bulk damaged adhesive. A comparison with the experimental data from Murakami et al. (2016) is presented.

Figure 6 highlights that β governs the softening behavior related to the damage accumulation until failure. As β decreases, the adhesive behavior evolves from quasi-brittle to brittle (see curve for $\beta = 0.01$ in Fig. 6).

4.2. Joint adhesive configuration

For the adhesive in the joint configuration, we assume a 1D approximation of a pure torsional test. By specializing Eq. (25) in the 1D case, the damage evolution law reads as:

$$\tilde{\eta}(R)\dot{R}^{\beta} = -\left\{ \tilde{\omega}_{,R}(R) + \frac{1}{2} G_{,R}(R) [[u]]_s^2 \right\}_-, \quad (30)$$

with $[[u]]_s = u_s t$ is the tangential jump in displacement, which is imposed in the proposed numerical simulations. If the damaging material model by Welemane and Goidescu (2010) is assumed, $G_{,R}(R) = -2\pi G_0$ with G_0 the shear modulus of the undamaged adhesive. For the sake of simplicity, also in this configuration, it is assumed that $\tilde{\omega}_{,R}(R)$ and $\tilde{\eta}(R)$ are constant parameters, equal to $\tilde{\omega}_{,R}(R) = \tilde{\omega} = 1$

Accepted Manuscript

Pa/m, $\tilde{\eta}(R) = \bar{\eta} = 2 \cdot 10^3$ Pa·s/m. The joint adhesive it is assumed to be initially undamaged $R_0 = 0$, and we focus on the influence of the damage velocity β.

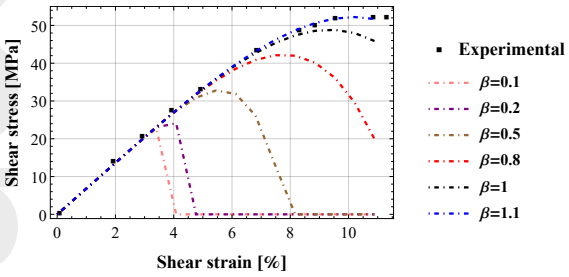

Figure 7: Influence of the damage velocity β: Torsional test behaviour of a damaged adhesive joint. A comparison with the experimental data from Murakami et al. (2016) is presented.

Figure 7 shows the global response (shear stress-strain) during a torsional test on Denatite 2204 adhesive in joint configuration (Murakami et al. (2016)). The experimental data are compared with the numerical results for varying β. For $\beta = 1.1$ a very good agreement is found. As before, the damage velocity β also affects the brittle behaviour of adhesive joint.

4.3. Damage rate-independent case

The damage rate-independent case is the limit case for a vanishing damage velocity β. In the bulk configuration, by replacing $\beta = 0$ in Eq. (26), it is obtained:

$$t = \frac{1}{\dot{\epsilon}} \left(\frac{\eta(R) + \omega_{,R}(R)}{\pi E_0} \right)^{\frac{1}{2}}. \tag{31}$$

In the joint configuration, by replacing $\beta = 0$ in Eq. (30), it is obtained:

$$t = \frac{1}{u_s} \left(\frac{\tilde{\eta}(R) + \tilde{\omega}_{,R}(R)}{\pi G_0} \right)^{\frac{1}{2}}. \tag{32}$$

Both equations (31) and (32) can be interpreted as a "correlation constraint" between the material functions $\tilde{\eta}$ and $\tilde{\omega}$ (or η and ω). Future work will be geared towards exploring this correlation. It is worth highlighting that when the parameters $\tilde{\eta}$ and $\tilde{\omega}$ (or η and ω) depend on $R(t)$, Eqs. (31) and (32) give an algebraic relation governing the evolution of the cracks density. On the contrary, when they are assumed constants, these relationships mean that the adopted damaged material model (Welemane and Goidescu (2010)) is not suitable in the rate-independent case, and other models should be explored.

5. Conclusion and perspectives

In this paper, a new generalized model of damaged imperfect interface is proposed.

Two novelties are introduced: (i) the non-local effect of the damage through the p-Laplacian of the damage variable R, which represents a cracks density; (ii) a rate-dependent effect through a damage velocity β. The resulting imperfect interface law is of the nonlinear-spring type due to the dependence on the damage. The interface stiffness takes into account the evolution of the damage variable. This evolution is managed by a nonlinear differential equation based on the generalized standard material model. Soft and hard imperfect interface cases are explored.

A parametric analysis on the damage velocity β is proposed on simple 1D numerical examples in both bulk and joint adhesive configurations. The role and relevance of the damage velocity is illustrated through a comparison with experimental data taken from literature. The numerical results show how the mechanical properties of the bulk adhesive and the joint degrade as damage evolves, indicating a transition from quasi-brittle to brittle behavior as the damage velocity decreases. As a perspective, it will be interesting to explore the correlations between the three damage parameters: activation energy threshold ω, viscosity η and velocity β. To this aim, an extensive parametric analysis is necessary. Moreover, the study should be completed by investigating the dependency of these parameters on the damage variable R.

We also plan to implement the model in a computational software to study complex bonding geometries and to compare them with experimental results. We will also study the consistency of the model (existence and uniqueness of the solution) and its behaviour in the presence of uncertainties, as proposed in Bauzet, Bonetti, Bonfanti, Lebon and Vallet (2017).

CRediT authorship contribution statement

Frédéric Lebon: Conceptualization, Theoretical developments Methodology, Writing - Original Draft. **Maria Letizia Raffa:** Methodology, Software development, Validation, Visualization, Writing - Review & Editing. **Raffaella Rizzoni:** Methodology, Software development, Visualization, Writing - Review & Editing.

References

Amaechi, C., Chesterton, C., Butler, H., Wang, F., Ye, J., 2021. Ocean Eng. 242, 110062.
Ascione, F., Mancusi, G., Spadea, S., Lamberti, M., Lebon, F., Maurel-Pantel, A., 2015. Comp. Struct. 131, 55.
Bauzet, C., Bonetti, E., Bonfanti, G., Lebon, F., Vallet, G., 2017. Math. Meth. Appl. Sci. 40, 5241.
Benveniste, Y., Miloh, T., 2001. Mech. Mat. 33, 309.
Bonetti, E., Bonfanti, G., Lebon, F., Rizzoni, R., 2017. Meccanica 52, 1911.
Budhe, S., Banea, M., de Barros, S., 2018. Appl. Adh. Sci. 6, 3.
Budzik, M., Wolfahrt, M., Reis, P., Kozlowski, M., Sena-Cruz, J., Papadakis, L., Saleh, M., Machalicka, K., de Freitas, S.T., Vassilopoulos, A., 2021. J. Adh. doi:doi/10.1080/00218464.2021.1953479.
Chaves, F., da Silva, L., de Moura, M., Dillard, D., Esteves, V., 2014. J. of Adh. 90, 955.
Delzendehrooy, F., Akhavan-Safar, A., Barbosa, A., Beygi, R., Cardoso, D., Carbas, R., Marques, E., da Silva, L., 2022. Comp. Struct. 268, 115490.

Accepted Manuscript

Dumont, S., Lebon, F., Raffa, M., Rizzoni, R., 2017. Ann. Sol. Struct. Mech. 9, 13.
Farrar, D., 2012. Int. J. Adh. Adhesives 33, 89.
Furtsev, A., Rudoy, E., 2020. Int. J. Sol. Struct. 202, 562.
Geymonat, G., Krasucki, F., Lenci, S., 1999. Math. Mech. Sol. 16, 201.
Hochard, C., Lahellec, N., Bordreuil, C., 2007. Comp. Struct. 80, 321.
Hochard, C., Payan, J., Bordreuil, C., 2006. A progressive first ply failure model for woven ply cfrp laminates under static and fatigue loads. Int. J. Fatigue 28, 1270.
Kupski, J., de Freitas, S.T., 2021. Comp. Struct. 268, 113923.
Lamberti, M., Maurel-Pantel, A., Ascione, F., Lebon, F., 2016. Comp. Struct. 147, 247.
Lamberti, M., Maurel-Pantel, A., Lebon, F., Ascione, F., 2022. Comp. Struct. 279, 114741.
Licht, C., Orankitjaroen, S., Weller, T., 2022. Compt. R. Mec. 350, 27.
Maitlo, A., Lebon, F., Bauzet, C., 2019. J. of Multiscale Model. 10, 1841001.
Maurel-Pantel, A., Lamberti, M., Raffa, M., Suarez, C., Ascione, F., Lebon, F., 2019. Comp. Struct. 10, 1841001.
Maurer, P., Bekes, K., Gernhardt, C., Schaller, H., Schubert, J., 2004. Int. J. Oral and Maxillofacial Surg. 33, 377.
Meerbeek, B.V., Peumans, M., Poitevin, A., Mine, A., Ende, A.V., Neves, A., Munck, J.D., 2010. Dent. Mat. 26, 100.
Murakami, S., Sekiguchi, Y., Sato, C., Yokoi, E., Furusawa, T., 2016. Int. J. Adh. Adhes. 67, 86–93.
Orefice, A., Mancusi, G., Dumont, S., Lebon, F., 2016. Technologies 4, 20.
Raffa, M., Lebon, F., Rizzoni, R., 2022. Int. J. Mech. Sci. 216, 106974.
Raffa, M., Rizzoni, R., Lebon, F., 2021. Technol. 9(1), 19.
Ramalho, L.D.C., Campilho, R.D.S.G., Belinha, J., Silva, L.F M.D., 2020. Static strength prediction of adhesive joints: A review. Int. J. Adh. Adhesives 96, 102451.
Rizzoni, R., Dumont, S., Lebon, F., Sacco, S., 2014. Higher order model for soft and hard interfaces. Int. J. Sol. Struct. 51, 4137.
Serpilli, M., Lenci, S., 2012a. Int. J. Sol. Struct. 49, 1147.
Serpilli, M., Lenci, S., 2012b. Int. J. Sol. Struct. 81, 130.
Weber, S., Chapman, M., 1984. Clin. Ortho. Rel. Res. 191, 249.
Welemane, H., Goidescu, C., 2010. Comptes R. Mec. 338, 271.

Frédéric Lebon Writing - Review & Editing Conceptualization Methodology

Maria Letizia Raffa Writing - Review & Editing Methodology Software

Raffaella Rizzoni Writing - Review & Editing Methodology Conceptualization

Accepted Manuscript